

Photocatalysis

La₅Ti₂Cu_{0.9}Ag_{0.1}S₅O₇ Modified with a Molecular Ni Catalyst for Photoelectrochemical H₂ GenerationTimothy E. Rosser,^[a, b] Takashi Hisatomi,^[a, e] Song Sun,^[a, c] Daniel Antón-García,^[b] Tsutomu Minegishi,^[a] Erwin Reisner,^{*[b]} and Kazunari Domen^{*[a, d]}

Abstract: The stable and efficient integration of molecular catalysts into *p*-type semiconductor materials is a contemporary challenge in photoelectrochemical fuel synthesis. Here, we report the combination of a phosphonated molecular Ni catalyst with a TiO₂-coated La₅Ti₂Cu_{0.9}Ag_{0.1}S₅O₇ photocathode for visible light driven H₂ production. This hybrid assembly provides a positive onset potential, large photocurrents, and high Faradaic yield for more than three hours. A decisive feature of the hybrid electrode is the TiO₂ interlayer, which stabilizes the oxysulfide semiconductor and allows for robust attachment of the phosphonated molecular catalyst. This demonstration of an oxysulfide-molecular catalyst photocathode provides a novel platform for integrating molecular catalysts into photocathodes and the large photovoltage of the present system makes it ideal for pairing with photoanodes.

Splitting water into H₂ and O₂ with sunlight in a photoelectrochemical (PEC) cell holds great promise for sustainable fuel production.^[1,2] However, the limited availability of high-performance photocathodes that 1) utilize the long wavelengths of sunlight,^[3] 2) avoid photocorrosion in aqueous solution^[4,5] and 3) do not require precious metal co-catalysts^[6] remains a bottleneck for applications.

Oxysulfides La₅Ti₂CuS₅O₇ (LTC) and La₅Ti₂Cu_{0.9}Ag_{0.1}S₅O₇ (LTCA) have emerged as promising photocathode materials,^[7-9] with the latter absorbing light up until 710 nm and demonstrating

PEC H₂ production from aqueous solution, with an onset potential of 0.8 V versus the reversible hydrogen electrode (RHE) when using Pt as a co-catalyst.^[8] Surface modification of LTC and LTCA photocathodes with thin TiO₂ layers improves their activity due to enhanced charge separation,^[10,11] and layers of amorphous TiO₂ have been shown to protect LTCA under strongly alkaline (pH 13) conditions.^[12]

Molecular complexes of Earth-abundant metals are alternatives to precious metal nanoparticles, where tuning the primary and secondary coordination spheres allows obtaining very high per site activities.^[13] In addition, modification of the outer coordination shell of molecular catalysts allows for specific anchoring onto photocathode surfaces.^[14,15] Phosphonic acid anchoring groups have a high affinity for metal oxide surfaces under acidic and pH neutral aqueous conditions,^[16,17] and are thus well suited for immobilizing molecular catalysts to photocathodes stabilized with TiO₂ protection layers.^[18]

In this study, we report an LTCA photocathode that is stabilized by a sputtered TiO₂ layer and modified with a molecular H₂ evolution catalyst. As catalyst, we employ a Ni bis(diphosphine)-based complex (NiP, Figure 1), which shows optimal activity under mildly acidic conditions,^[19] and has previously been employed on a mesoporous TiO₂ electrode and a TiO₂-protected *p*-Si photocathode.^[20,21] The resulting LTCA|TiO₂|NiP photoelectrode represents a new type of molecular-semiconductor hybrid photocathode with high PEC performance and stability, as well as expanding the operating conditions of LTCA to acidic aqueous solution.

[a] Dr. T. E. Rosser, Prof. T. Hisatomi, Prof. S. Sun, Prof. T. Minegishi, Prof. K. Domen
Department of Chemical System Engineering, Faculty of Engineering
University of Tokyo, 7-3-1 Hongo, Bunkyo-ku, Tokyo 113-8656 (Japan)
E-mail: domen@chemsys.t.u-tokyo.ac.jp

[b] Dr. T. E. Rosser, D. Antón-García, Prof. E. Reisner
Christian Doppler Laboratory for Sustainable SynGas Chemistry
Department of Chemistry, University of Cambridge
Lensfield Road, Cambridge, CB2 1EW (UK)
E-mail: reisner@ch.cam.ac.uk

[c] Prof. S. Sun
National Synchrotron Radiation Laboratory
Collaborative Innovation Center of Chemistry for Energy Materials
University of Science & Technology of China
Hefei, Anhui 230029 (P. R. China)

[d] Prof. K. Domen
Center for Energy & Environmental Science, Shinshu University
4-17-1 Wakasato, Nagano-shi, Nagano 380-8553 (Japan)

[e] Prof. T. Hisatomi
Current affiliation: Center for Energy & Environmental Science
Shinshu University, 4-17-1 Wakasato, Nagano-shi
Nagano 380-8553 (Japan)

Supporting information and the ORCID identification numbers for the authors of this article can be found under:

<https://doi.org/10.1002/chem.201801169>. Additional data related to this publication are available at the University of Cambridge data repository: <https://doi.org/10.17863/CAM.23024>.

© 2018 The Authors. Published by Wiley-VCH Verlag GmbH & Co. KGaA. This is an open access article under the terms of the Creative Commons Attribution License, which permits use, distribution and reproduction in any medium, provided the original work is properly cited.



Part of a Special Issue focusing on topics within the field of renewable energy. To view the complete issue, visit Issue 69.

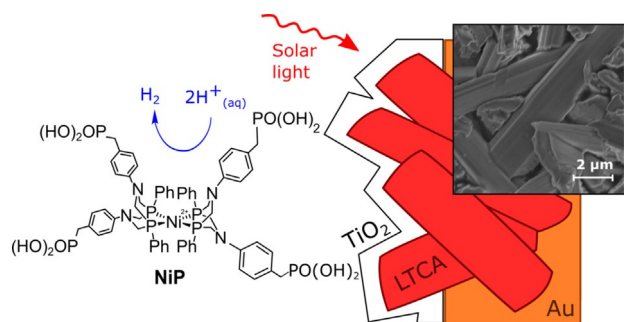


Figure 1. Schematic representation of solar-light driven reduction of aqueous protons to H_2 with the $\text{LTCA}|\text{TiO}_2|\text{NiP}$ photocathode. An SEM image of $\text{LTCA}|\text{TiO}_2|\text{NiP}$ is shown as inset.

Particulate LTCA was prepared as previously described,^[8,9] and was assembled into freestanding photocathodes with an Au backing layer. Nanostructured LTCA films were subsequently modified with a thin (approx. 2 nm) layer of TiO_2 by reactive RF magnetron sputtering, and annealed under air to form electrodes referred to herein as $\text{LTCA}|\text{TiO}_2$ (see Supporting Information for details). Sputtering was used because this technique has previously been shown to increase the activity of LTC and LTCA photocathodes by minimizing charge recombination.^[10,11] The TiO_2 layer also stabilizes the LTCA under the otherwise corrosive acidic conditions required for **NiP** to operate,^[19,22] as well as providing a proven attachment site for this catalyst.^[20,21] Scanning electron microscopy (SEM, Figure 1) of these electrodes shows the rod-like structure of the LTCA particles with lengths of approximately a few micrometers.

Immobilization of **NiP** on $\text{LTCA}|\text{TiO}_2$ electrodes was achieved by submersion in a methanol solution (0.5 mM) overnight. The presence of **NiP** was confirmed by the observation of N, P, and Ni in the XPS spectrum of the modified electrode (Figure S1 in Supporting Information). The **NiP** surface loading was quantified as $33.7 \pm 2.4 \text{ nmol cm}^{-2}$ by desorption from $\text{LTCA}|\text{TiO}_2$ in aqueous NaOH solution (0.1 M), followed by UV/Vis spectroscopic analysis (see Supporting Information).^[20] This value is in the expected range for a mesostructured electrode modified with a phosphonated metal complex.^[17,21]

The PEC properties of the $\text{LTCA}|\text{TiO}_2|\text{NiP}$ electrode were first studied in aqueous Na_2SO_4 solution at pH 3 under simulated solar irradiation ($\text{AM } 1.5\text{G}$, 100 mW cm^{-2}). The linear sweep voltammetry (LSV) scans shown in Figure 2a show a cathodic onset photocurrent at approximately 0.65 V versus RHE with a photocurrent of -0.6 mA cm^{-2} at 0 V versus RHE. Note that the LSV response does not represent an improvement compared to the $\text{LTCA}|\text{TiO}_2$ electrodes without catalyst modification on this timescale (approximately 1 min). This may be due to a photoreductive decomposition process occurring for $\text{LTCA}|\text{TiO}_2$, leading to initially higher but short-lived catalytic activity (see below).

Nevertheless, controlled potential photoelectrolysis (CPPE, Figure 2b) during irradiation at +0.3 V versus RHE reveals a different response between **NiP**-modified and bare $\text{LTCA}|\text{TiO}_2$ electrodes. The latter shows an initial photocurrent of -0.4 mA cm^{-2} , which decays quickly to zero within three

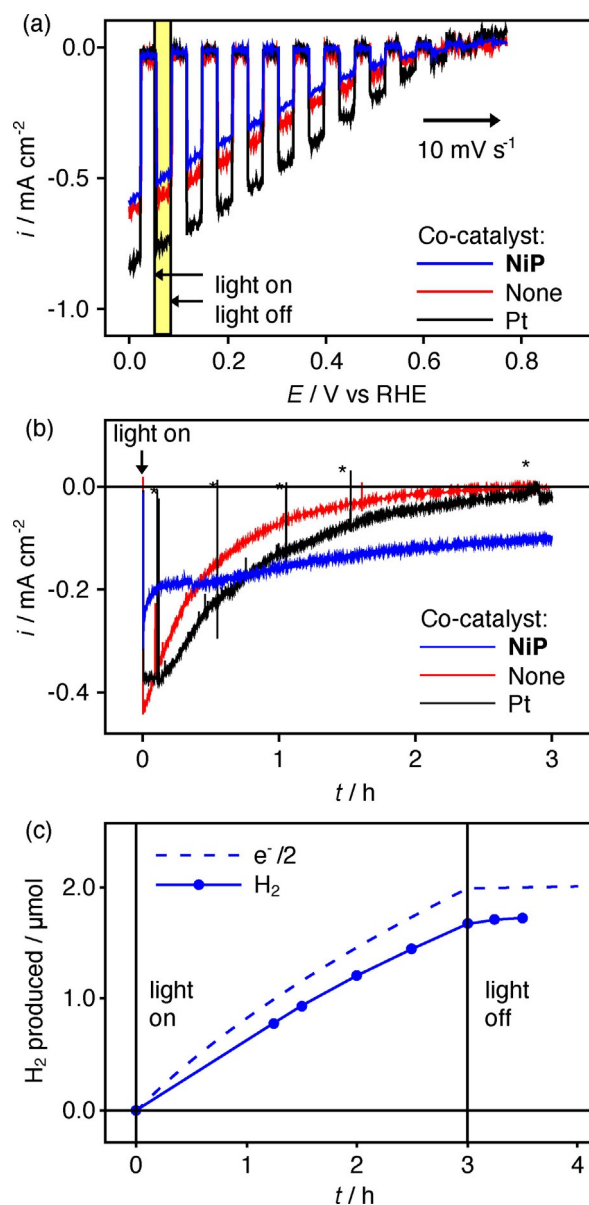


Figure 2. a) Light chopped LSV (scan rate = 10 mV s^{-1} , anodic direction) and b) CPPE at +0.3 V vs. RHE of $\text{LTCA}|\text{TiO}_2$ photocathodes modified with **NiP**, no co-catalyst or Pt (* indicates where irradiation was temporarily interrupted in CPPE) c) H_2 quantification for $\text{LTCA}|\text{TiO}_2|\text{NiP}$ from (b). The dashed line represents the theoretical amount of H_2 based on the charge passed (i.e., 100% Faradaic yield). Conditions: Aqueous Na_2SO_4 (0.1 M) at pH 3 electrolyte solution under simulated solar irradiation ($\text{AM } 1.5\text{G}$) and a constant Ar purge.

hours, indicating instability and/or lack of catalysis. In contrast, prolonged CPPE with $\text{LTCA}|\text{TiO}_2|\text{NiP}$ under the same conditions showed an initial photocurrent of -0.2 mA cm^{-2} , which was retained at 50% after 3 hours irradiation (Figure 2b). Product quantification through gas chromatography during a CPPE experiment with $\text{LTCA}|\text{TiO}_2|\text{NiP}$ reveals that $1.7 \mu\text{mol H}_2$ was produced, representing a turnover number (TON) of approximately 50 per initial Ni site. The Faradaic yield was measured to be 87% (Figure 2c), which matches the values obtained for previously reported **NiP** catalysts anchored on TiO_2 cathodes^[20] and photocathodes.^[21] Longer term CPPE (Figure S2 in Sup-

porting Information) demonstrated continued photocurrent for at least 6 h, although with a steadily declining activity that is consistent with catalyst desorption or degradation. In the absence of NiP, H₂ production had essentially ceased after 2 h (Figure S3 a), suggesting that this is accompanied by a degradation process that is avoided when the electrons are harvested by the NiP catalyst. It has previously been shown that NiP can efficiently accept electrons from the TiO₂ conduction band,^[19,20] which slows the otherwise rapid degradation of the LTCA semiconductor material.

The LTCA|TiO₂|NiP photocathodes were further characterized by measuring the single wavelength incident photon-to-current efficiencies (IPCE) across the visible spectrum with an applied potential of +0.3 V versus RHE. The photocathodes demonstrated photocathodic current at wavelengths as long as 660 nm, matching the diffuse reflectance UV/Vis spectrum (Figure 3). An IPCE of 2.4% was recorded at 440 nm.

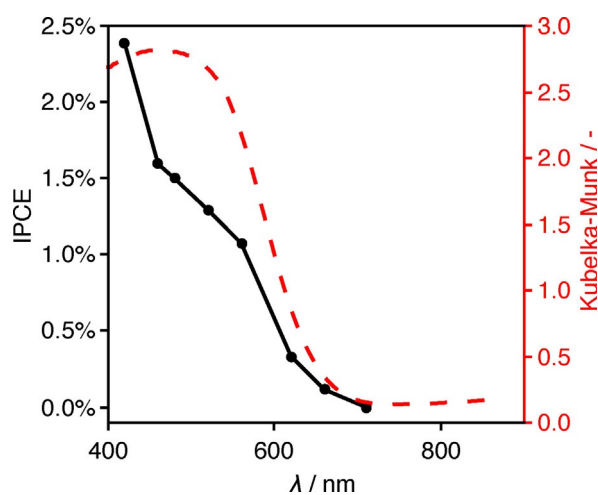


Figure 3. Black line: Incident photon-to-current efficiency (IPCE) spectrum of LTCA|TiO₂|NiP photocathode in pH 3 Na₂SO₄ (0.1 M) electrolyte solution irradiated with a 300 W Xe lamp fitted with narrow band filters under a purge of Ar and an applied potential of 0.3 V vs. RHE. Red dashed line: DRS UV/Vis spectrum of LTCA powder (in Kubelka–Munk absorbance units).

Analysis of immobilized NiP on the electrode surface after a three-hour CPPE experiment (quantified by UV/Vis spectroscopy following desorption in aqueous NaOH, see above) revealed a surface loading of 16 nmol cm⁻². This represents a loss of approximately half of the initial catalyst from the electrode surface during CPPE and matches the 50% drop in PEC activity (Figure 2 b). Moreover, a qualitative resemblance between the UV/Vis peaks of the desorbed NiP before and after CPPE (Figure S4), as well as retention of peaks corresponding to N and P in the XPS spectra after 1 h CPPE (Figure S1), support the molecular integrity of NiP during the PEC experiments. Ni signals belonging to either NiP or a decomposition product could not be clearly resolved in the post-CPPE XPS spectra.

Control experiments were performed without a sputtered TiO₂ layer. A NiP loading of 17.6 ± 3.5 nmol cm⁻² was determined for LTCA|NiP, which is approximately half that observed for LTCA|TiO₂|NiP, and thus in agreement with the particular

affinity between the phosphonate-modified molecules and TiO₂.^[15,23] Moreover, when these electrodes were subjected to CPPE at +0.3 V versus RHE under the same conditions as described above (Figure S5), the initially low photocurrent of -0.15 mA cm⁻² approached zero within two hours, demonstrating the requirement for a stabilizing layer. Thus, TiO₂ adds two further benefits to the increase in photocurrent observed at pH 10^[10,11]—it stabilizes LTCA and provides an improved anchoring site for NiP.

LTCA|TiO₂ electrodes modified with Pt instead of NiP were prepared by PEC reduction of H₂PtCl₆ (see Supporting Information for details). When studied in pH 10 electrolyte solution, the most commonly used conditions for these materials,^[8] the electrodes displayed a photocurrent of -1.0 mA cm⁻² at 0 V versus RHE in the LSV and relatively stable H₂ production for two hours at E_{appl} = +0.5 V versus RHE (Figure S6). In pH 3 electrolyte solution, the LSV of the LTCA|TiO₂|Pt electrodes displayed a similar onset potential to LTCA|TiO₂|NiP electrodes with photocurrent reaching -0.8 mA cm⁻² at 0 V versus RHE (Figure 2 a). However, CPPE at +0.3 V versus RHE showed a much quicker decay than with the LTCA|TiO₂|NiP electrodes, falling to only -0.01 mA cm⁻² after three hours irradiation and a Faradaic yield of 84% (Figure 2 b and Figure S3 b). This decay is consistent with previous studies, where the contact between this TiO₂ protecting layer and the Pt catalyst has limited the durability of the photocathode,^[24] and either an additional Mo/Ti layer^[25] or replacing the Pt co-catalyst with a thick RuO_x film^[26] has been required to achieve long term performance. Our photoelectrode therefore provides a rare example where the chemical attachment between a molecular catalyst and the electrode is improved compared to a precious metal catalyst layer, and indeed the molecular catalyst appears essential for operation of the LTCA material under mildly acidic conditions. H₂ production by LTC or LTCA from acidic solution has not previously been demonstrated, and therefore the use of both the TiO₂ stabilizing layer and molecular catalyst expands the possible operating conditions of this class of material.

This work represents an advance in the assembly of hybrid semiconductor/molecular catalyst photocathodes due to its positive operating potential and long wavelength activity. The onset potential of +0.65 V versus RHE is significantly more positive than for p-Si modified with TiO₂ and the same NiP co-catalyst,^[21] and is comparable to the values reported using GaP-based hybrid photocathodes.^[27,28] Additionally, our LTCA hybrid photocathodes allow H₂ production up to λ = 660 nm, which exceeds that of GaP, where the band gap limits light absorption to 549 nm.^[14] The use of the particle transfer fabrication method, compared to flat semiconductor wafers such as p-Si and GaP, makes this electrode scaffold potentially scalable over large areas. The excellent contact between the particles and the contact layer (Au in this case) removes the requirement for high crystallinity across the whole panel,^[29,30] and the intrinsically mesostructured surface enables high catalyst loading. However, the loss of activity is somewhat faster than for the previous (photo)cathodes using the same catalyst.^[20,21] Previous systems utilized mesoporous TiO₂ with several-μm-thick films, which trap the catalyst through re-adsorption following

desorption, when compared to the nm-thick TiO₂ layer reported here. Therefore, increasing the porosity of the TiO₂ layer may improve the system's longevity in future development. Finally, LTCA|TiO₂|NiP compares favourably in terms of photocurrent and Faradaic yield with "all-molecular" dye/H₂-catalyst assemblies, which are typically immobilised on *p*-type materials such as NiO and CuCrO₂.^[31–35]

In conclusion, photocathodes based on the oxysulfide La₅Ti₂Cu_{0.9}Ag_{0.1}S₃O₇ were combined with a molecular catalyst, enabling early-onset H₂ fuel synthesis with a molecular/inorganic hybrid. This was accomplished by employing a sputtered TiO₂ layer, which protects the material from the aqueous electrolyte solution and provides a suitable attachment site for the phosphonic acid-modified molecular catalyst NiP. The latter was crucial for the high performance of the photocathode, which still retained 50% of its initial activity after three hours photoelectrolysis. An analogous photocathode modified with Pt displayed poor stability, giving a rare example where a molecular catalyst exceeds the activity and stability of Pt for H₂ production.^[36] Our results demonstrate the possibility of replacing expensive Pt with a first row transition metal catalyst for oxysulfide-type photocathode materials. The use of a TiO₂ overlayer opens up their use in previously unreported acidic conditions that may be required in tandem PEC device architectures. From a molecular catalysis point of view, this is the most positive operating potential for an inorganic light-harvester/molecular catalyst hybrid, and the system retains high Faradaic efficiency even at this potential. This is therefore an essential step towards constructing an efficient, bias-free molecule-catalysed photoelectrochemical cell.

Experimental Section

Experimental details can be found in the Supporting Information.

Acknowledgements

This work was supported by an Overseas Researcher Postdoctoral Fellowship from the Japan Society for the Promotion of Science (JSPS) (to T.E.R.), the Christian Doppler Research Association (Austrian Federal Ministry of Science, Research, and Economy and the National Foundation for Research, Technology and Development), and the OMV group (to E.R.), the EPSRC (Ph.D. scholarship to D.A.G.) and by Grants-in-Aids for Scientific Research (A) (No. 16H02417) and for Young Scientists (A) (No. 15H05494) from JSPS. The authors wish to thank Yosuke Kageshima of the University of Tokyo for kind assistance with the Faradaic efficiency measurements.

Conflict of interest

The authors declare no conflict of interest.

Keywords: hydrogen • molecular electrochemistry • semiconductors • solar fuels • surface chemistry

- [1] J. R. McKone, N. S. Lewis, H. B. Gray, *Chem. Mater.* **2014**, *26*, 407–414.
- [2] M. S. Prévot, K. Sivula, *J. Phys. Chem. C* **2013**, *117*, 17879–17893.
- [3] H. Kaneko, T. Minegishi, M. Nakabayashi, N. Shibata, Y. Kuang, T. Yamada, K. Domen, *Adv. Funct. Mater.* **2016**, *26*, 4570–4577.
- [4] M. Crespo-Quesada, E. Reisner, *Energy Environ. Sci.* **2017**, *10*, 1116–1127.
- [5] B. Seger, T. Pedersen, A. B. Laursen, P. C. K. Vesborg, O. Hansen, I. Chorkendorff, *J. Am. Chem. Soc.* **2013**, *135*, 1057–1064.
- [6] C. G. Morales-Guio, L. Liardet, M. T. Mayer, S. D. Tilley, M. Grätzel, X. Hu, *Angew. Chem. Int. Ed.* **2015**, *54*, 664–667; *Angew. Chem.* **2015**, *127*, 674–677.
- [7] J. Liu, T. Hisatomi, G. Ma, A. Iwanaga, T. Minegishi, Y. Moriya, M. Katayama, J. Kubota, K. Domen, *Energy Environ. Sci.* **2014**, *7*, 2239–2242.
- [8] T. Hisatomi, S. Okamura, J. Liu, Y. Shinohara, K. Ueda, T. Higashi, M. Katayama, T. Minegishi, K. Domen, *Energy Environ. Sci.* **2015**, *8*, 3354–3362.
- [9] S. Sun, T. Hisatomi, Q. Wang, S. Chen, G. Ma, J. Liu, S. Nandy, T. Minegishi, M. Katayama, K. Domen, *ACS Catal.* **2018**, *8*, 1690–1696.
- [10] J. Liu, T. Hisatomi, D. H. K. Murthy, M. Zhong, M. Nakabayashi, T. Higashi, Y. Suzuki, H. Matsuzaki, K. Seki, A. Furube, N. Shibata, M. Katayama, T. Minegishi, K. Domen, *J. Phys. Chem. Lett.* **2017**, *8*, 375–379.
- [11] J. Liu, T. Hisatomi, M. Katayama, T. Minegishi, K. Domen, *ChemPhotoChem* **2018**, *2*, 234–239.
- [12] T. Higashi, Y. Shinohara, A. Ohnishi, J. Liu, K. Ueda, S. Okamura, T. Hisatomi, M. Katayama, H. Nishiyama, T. Yamada, T. Minegishi, K. Domen, *ChemPhotoChem* **2017**, *1*, 167–172.
- [13] M. L. Helm, M. P. Stewart, R. M. Bullock, M. Rakowski Dubois, D. L. DuBois, *Science* **2011**, *333*, 863–866.
- [14] D. Khusnutdinova, A. M. Beiler, B. L. Wadsworth, S. I. Jacob, G. F. Moore, *Chem. Sci.* **2017**, *8*, 253–259.
- [15] J. Willkomm, K. L. Orchard, A. Reynal, E. Pastor, J. R. Durrant, E. Reisner, *Chem. Soc. Rev.* **2016**, *45*, 9–23.
- [16] E. Bae, W. Choi, *J. Phys. Chem. B* **2006**, *110*, 14792–14799.
- [17] N. M. Muresan, J. Willkomm, D. Mersch, Y. Vaynzof, E. Reisner, *Angew. Chem. Int. Ed.* **2012**, *51*, 12749–12753; *Angew. Chem.* **2012**, *124*, 12921–12925.
- [18] B. Mei, T. Pedersen, P. Malacrida, D. Bae, R. Frydendal, O. Hansen, P. C. K. Vesborg, B. Seger, I. Chorkendorff, *J. Phys. Chem. C* **2015**, *119*, 15019–15027.
- [19] M. A. Gross, A. Reynal, J. R. Durrant, E. Reisner, *J. Am. Chem. Soc.* **2014**, *136*, 356–366.
- [20] T. E. Rosser, M. A. Gross, Y.-H. Lai, E. Reisner, *Chem. Sci.* **2016**, *7*, 4024–4035.
- [21] J. J. Leung, J. Warnan, D. H. Nam, J. Z. Zhang, J. Willkomm, E. Reisner, *Chem. Sci.* **2017**, *8*, 5172–5180.
- [22] A. Reynal, E. Pastor, M. A. Gross, S. Selim, E. Reisner, J. R. Durrant, *Chem. Sci.* **2015**, *6*, 4855–4859.
- [23] C. Queffelec, M. Petit, P. Janvier, D. A. Knight, B. Bujoli, *Chem. Rev.* **2012**, *112*, 3777–3807.
- [24] A. Paracchino, N. Mathews, T. Hisatomi, M. Stefiik, S. D. Tilley, M. Grätzel, *Energy Environ. Sci.* **2012**, *5*, 8673–8681.
- [25] H. Kumagai, T. Minegishi, N. Sato, T. Yamada, J. Kubota, K. Domen, *J. Mater. Chem. A* **2015**, *3*, 8300–8307.
- [26] S. D. Tilley, M. Schreier, J. Azevedo, M. Stefiik, M. Graetzel, *Adv. Funct. Mater.* **2014**, *24*, 303–311.
- [27] A. M. Beiler, D. Khusnutdinova, S. I. Jacob, G. F. Moore, *ACS Appl. Mater. Interfaces* **2016**, *8*, 10038–10047.
- [28] A. M. Beiler, D. Khusnutdinova, B. L. Wadsworth, G. F. Moore, *Inorg. Chem.* **2017**, *56*, 12178–12185.
- [29] T. Minegishi, N. Nishimura, J. Kubota, K. Domen, *Chem. Sci.* **2013**, *4*, 1120–1124.
- [30] H. Kumagai, T. Minegishi, Y. Moriya, J. Kubota, K. Domen, *J. Phys. Chem. C* **2014**, *118*, 16386–16392.
- [31] N. Kaefter, J. Massin, C. Lebrun, O. Renault, M. Chavarot-Kerlidou, V. Artero, *J. Am. Chem. Soc.* **2016**, *138*, 12308–12311.
- [32] M. A. Gross, C. E. Creissen, K. L. Orchard, E. Reisner, *Chem. Sci.* **2016**, *7*, 5537–5546.
- [33] F. Li, K. Fan, B. Xu, E. Gabrielsson, Q. Daniel, L. Li, L. Sun, *J. Am. Chem. Soc.* **2015**, *137*, 9153–9159.

- [34] P. Meng, M. Wang, Y. Yang, S. Zhang, L. Sun, *J. Mater. Chem. A* **2015**, *3*, 18852–18859.
- [35] C. E. Creissen, J. Warnan, E. Reisner, *Chem. Sci.* **2018**, *9*, 1439–1447.
- [36] B. C. M. Martindale, G. A. M. Hutton, C. A. Caputo, E. Reisner, *J. Am. Chem. Soc.* **2015**, *137*, 6018–6025.

Manuscript received: March 7, 2018

Accepted manuscript online: May 11, 2018

Version of record online: June 6, 2018
